

SAR image change detection using distance between distributions of classes

Grégoire Mercier

GET/ENST Bretagne, dpt ITI,
TAMCIC, équipe TIME, FRE 2658,
Technopôle Brest-Iroïse, CS 83818,
F-29238 Brest Cedex, France.
Email: gregoire.mercier@enst-bretagne.fr

Stéphane Derrode

EGIM, groupe GSM, Institut Fresnel, UMR 6133
Domaine Universitaire de Saint Jérôme,
F-13013 Marseille Cedex 20, France.
Email: stephane.derrode@egim-mrs.fr

Abstract—The problem of detecting abrupt changes in a set of Synthetic Aperture Radar (SAR) images is carried out by comparing the results of segmentation between images with different modalities acquired before and after a disaster. Individual segmentations are not considered by themselves since they yield surface map characterization while the goal is to detect a temporal evolution of soil characteristics. Hence, we propose to use the modification of class statistics in the images in order to characterize potential changes and to prevent from false alarms that may be induced by the specific modality of each SAR acquisition.

The change detection process is divided in two steps: 1) segmentation of the observations in order to have an estimation of the marginal probability distribution function (pdf) of each class; 2) comparison of the pdf from different images to detect changes by means of evidential and paradoxical reasoning.

This two-stages process has been applied on Radarsat images (F2 and F5) of the Nyiragongo volcano, DR Congo, erupted on January 2002. The results obtained outperform simple strategies based on image differencing/ratioing.

I. INTRODUCTION

Satellite remote sensing change detection of the Earth surface is a central task for many kinds of monitoring purposes. It uses temporal series of images taken on the same geographical area at different dates. These changes can be divided coarsely in two types :

- *slow and thin changes* like seasonal vegetation change or the evolution of rotations in agriculture, in which case it is necessary to have a time series of images to detect these evolutions;
- *spectacular and fast changes* like damages due to a natural disaster (earthquake, flood) or of anthropic origin (deforestation, forest fire), and, in this case, two images acquired before and after the event can be enough.

In this work, we are mainly concerned with the second type, qualified as abrupt, which does not mean of big scale but rather instantaneous.

In the past years, most of the proposed change detection techniques has been devoted to the analysis of mono- and multi-spectral optical data and for specific change detection applications [1]–[4]. It is however clear that the intrinsic limits of these sensors, in particular their dependence to weather conditions, are particularly constraining and not very realistic

within an operational framework. This is the case of the cartography of damages caused by a major natural disaster (eruption, flood, ...) during the period of crisis management .

The recent state of the art from P. Coppin *et al.* [5] underlines the deficiencies in the use of radar data for thematic applications of change detection. Indeed, studies related to satellite-based SAR imagery are much fewer and more recent [6]–[10]. Due to their all-weather mapping capability, these sensors hold a strong potential for change detection studies and can guaranty operational systems also in presence of critical atmospheric circumstances and night conditions of illumination. Furthermore, during the period just after a disaster, all the information available must be use, even if the first operational acquisition comes from a radar. However, the problem of automatic detection of changes is made more difficult, mainly for the following reasons:

- the image modality with the presence of speckle inherent to the backscattering mechanisms;
- the incidence (angle of sight and ascending/descending orbits) of the two images acquired by the sensor;
- problems related to the difference in generation of radar sensors, problem which can occur when the two images are separated from several years (spatial resolution, inter-calibration, ground segment, final product...);
- the “natural” evolution of the observed scene (slow phenomenon) should not be confused with abrupt changes (fast phenomenon) we are looking for.

Hence, there is a need for the development of change detection methodologies adapted to SAR imagery. Basically, change detection techniques rely on some clustering schemes that identify the coordinates of pixels that have changed between two dates. There is loosely three sets of methods :

- the classification of some feature maps, such as image differencing or ratioing, selective PCA [2] or mutual information [11], into ‘change’ and ‘no-change’ classes;
- the comparison of the individual classifications (Post Comparison classification) to identify changed areas [12];
- the direct and joint multirate classification of the pair of images [9], [13]. Classes where changes are occurring are expected to present statistics significantly different from

where change did not take place.

In this paper, we propose a novel strategy that consists in combining several unsupervised classification of SAR images that have been geometrically corrected and co-registered. The proposed technique is based on comparisons of pdf issued from the segmentations. Those comparisons take into consideration the difference of point of view from the sensors and give some candidates of ground change.

II. IMAGE MAPPING

Lets consider two SAR images I_{t_0} and I_{t_1} acquired before and after an event. It is assumed that the images are registered and each pixel is co-located even if the geometry differs from one image to the other. The change detection technique starts by performing classification of each image. The classifications yield ground state maps that will be used in a stochastic point of view to perform change detection.

A. Mixture estimation through SEM

A contextual Stochastic-Estimation-Maximization (SEM) method is used to perform a mixture estimation of K classes of the initial image (I_{t_0}). Each class ω_k ($0 \leq k < K$) is characterized through a Gaussian probability density function (pdf) $f^{t_0}(x_{t_0}|\omega_k)$. The classification by itself is defined by a posteriori condition:

$$\mathcal{C}_{t_0}(i, j) = \omega_{k_0} \quad \text{if:} \quad \forall k \in \{0, \dots, K\}, \text{ and } k \neq k_0 \\ f^{t_0}(I_{t_0}(i, j)|\omega_{k_0}) \geq f^{t_0}(I_{t_0}(i, j)|\omega_k)$$

for all pixels (i, j) .

A similar SEM mixture estimation is apply to the other image, that yields a set of K' pdf: $f^{t_1}(x_{t_1}|\omega'_\ell)$, $0 \leq \ell < K'$. At this point, it is of interest to consider the result of classification at t_0 to initialize the SEM estimation at t_1 . Furthermore, some extra classes have to be considered to characterize any ground evolution. The procedure to initialize SEM on image I_{t_1} by creating new classes is the following: we start by assuming $K' = K$, and, for $0 \leq \ell < K$

- 1) consider the histogram of I_{t_1} restricted to pixels (i, j) so that $\mathcal{C}_{t_0}(i, j) = \omega_\ell$.
- 2) while the histogram appears multimodal, split it by creating a new class $\omega_{K'}$. Increment K' .

Multimodality test is achieved by using zero-crossing of the first derivative of the empirical histogram.

B. Joint estimation

The SEM algorithm is also applied to the couple of images (I_{t_0}, I_{t_1}) in order to take into consideration the evolution of laws induced by the difference of the acquisition conditions. This vectorial SEM is performed in a way similar to the scalar SEM by considering 2D Gaussian laws. The SEM yields a set of pdf characterizing each classe ω''_ℓ , $0 \leq \ell < K'$: $f^{t_0, t_1}(x_{t_0}, x_{t_1}|\omega''_\ell)$. The initialization uses the classification \mathcal{C}_{t_1} with K' classes. Then, considering the two observations together, the couple of 1D pdf $\left(f^{t_0, t_1}_{|t_0}(x_{t_0}|\omega''_\ell), f^{t_0, t_1}_{|t_1}(x_{t_1}|\omega''_\ell)\right)$ integrates the evolution of pdf induced by the difference of

point of view from the sensors and also the evolution of pdf induced by the ground itself.

III. CHANGE SIGNATURES

Two points of view may be adapted to characterize some change signatures from the image map segmentations. The first one characterizes globally the evolution of the statistics; the other takes care of the pixel realizations in a stochastic point of view.

A. Distance between distributions

Lets consider the Battacharyya distance between two pdf f and g , which is defined as: $\int \sqrt{f(x)g(x)} dx$. We define the following change detection criteria :

$$\mathcal{D}(f, g) = 1 - \int \sqrt{f(x)g(x)} dx.$$

This criteria is based on the evolution of the pdf : it grows to 1 to express a difference between the two pdf, and decreases to 0 when the distributions remain similar. It is necessary to point out that \mathcal{D} is linked to an evolution of pdf that may be induced by ground modifications but also by sensor parameters.

B. Pixel point of view

Lets define a criteria dedicated to pixels' behavior. If a pixel remains the same while the pdf of its class has changed, its membership to the class will differ; also if a pixel has changed between the two acquisitions while the pdf of its class has not been modified dramatically, its membership will differ also. Then a significance measurement of a pixel (i, j) for images I and I' may be defined through the pdf f_I and $g_{I'}$ as:

$$\mathcal{S}_{(f_I, g_{I'})}(i, j) = f_I(I(i, j)) g_{I'}(I'(i, j)).$$

Furthermore, a contrast measurement may be defined to induce a potential change of the pixel (i, j) . The membership change of a pixel (i, j) between two images I and I' is defined through a contrast measure between the two pdf f_I and $g_{I'}$ as:

$$\rho_{(f_I, g_{I'})}(i, j) = 1 - \min\left(\frac{f_I(I(i, j))}{g_{I'}(I'(i, j))}, \frac{g_{I'}(I'(i, j))}{f_I(I(i, j))}\right).$$

Those measures characterize the evolution of the classes' pdf and the evolution of each pixel into its class. For change detection application, lets consider them between the segmentations of I_{t_0} and I_{t_1} and the pdf: $f^{t_0}(x_0|\omega_k)$, $f^{t_1}(x_1|\omega'_\ell)$ and the two components of the 2D pdf $f^{t_0, t_1}(x_0, x_1|\omega''_\ell) = \left(f^{t_0, t_1}_{|t_0}(x_{t_0}|\omega''_\ell), f^{t_0, t_1}_{|t_1}(x_{t_1}|\omega''_\ell)\right)$. Those evolutions are not necessary linked to ground change but give potential candidates to ground evolution. That is why those indicators are to be considered into an evidential and paradoxical reasoning.

IV. CHANGE DETECTION WITH PARADOXICAL THEORY

A. Dezert-Smarandache theory

The Dezert-Smarandache (DSm) theory can be considered as a generalization of the Dempster-Shafer (DS) one. In this new theory, the rule of combination takes into account both uncertain and paradoxical information [14]. Let consider the simplest frame of discernment $\Theta = \{\theta_{\text{ch}}, \theta_{\text{no ch}}\}$ involving only two elementary hypotheses ('change' and 'no change'), with no more additional assumptions on θ_{ch} and $\theta_{\text{no ch}}$. DSm theory deals with new basic belief assignments $m(\cdot) \in [0, 1]$ in accepting the possibility for paradoxical information such that:

$$m(\theta_{\text{ch}}) + m(\theta_{\text{no ch}}) + m(\theta_{\text{ch}} \cup \theta_{\text{no ch}}) + m(\theta_{\text{ch}} \cap \theta_{\text{no ch}}) = 1. \quad (1)$$

Θ denotes the finite set for exhaustive elements. The power set 2^Θ will be defined through the DS theory by: $2^\Theta = \{\emptyset, \theta_{\text{ch}}, \theta_{\text{no ch}}, \theta_{\text{ch}} \cup \theta_{\text{no ch}}\}$. The DSm theory introduce the notion of hyper-power set D^Θ through all composite propositions from elements of Θ with \cup and \cap operators such that: $D^\Theta = \{\emptyset, \theta_{\text{ch}} \cap \theta_{\text{no ch}}, \theta_{\text{ch}}, \theta_{\text{no ch}}, \theta_{\text{ch}} \cup \theta_{\text{no ch}}\}$. This constitutes what is called *free DSm model* $\mathcal{M}^f(\Theta)$ and allows to work with fuzzy concepts which own a continuous and relative intrinsic nature. However, when elements θ_i are truly exclusive, the hyper-power set D^Θ reduces naturally to the power set 2^Θ and the free DSm model goes down to the Shafer's model $\mathcal{M}^0(\Theta)$. However, between the free DSm model $\mathcal{M}^f(\Theta)$ and the Shafer's model $\mathcal{M}^0(\Theta)$, *hybrid model* may be defined to introduce exclusivity constraints and non existential constraints.

The generalized belief and plausibility functions are defined in almost the same manner as within the DS, *i.e.*

$$\text{Bel}(A) = \sum_{\substack{B \subseteq A \\ B \in D^\Theta}} m(B) \quad \text{and} \quad \text{Pl}(A) = \sum_{\substack{B \cap A \neq \emptyset \\ B \in D^\Theta}} m(B),$$

while the classic DSm rule of combination between two sources of evidences \mathcal{B}_1 and \mathcal{B}_2 follows:

$$\forall C \in D^\Theta, \quad m(C) = [m_1 \oplus m_2](C) = \sum_{\substack{A, B \in D^\Theta \\ A \cap B = C}} m_1(A) m_2(B).$$

B. Mass belief assignment

Lets consider first the comparison between the two SEM. A ground evolution may be expected at a pixel of position (i, j) when the distance between the two pdf $\mathcal{D}(f^{t_0}(I_{t_0}(i, j)|\omega), f^{t_1}(I_{t_1}(i, j)|\omega'))$ and the contrast between the membership values $\rho(f^{t_0}(I_{t_0}(i, j)|\omega), f^{t_1}(I_{t_1}(i, j)|\omega'))$ become significant. Furthermore, the decision may be taken when there is a contradiction between the distance and the contrast indicators. Then, we propose in table I the mass assignment for comparing I_{t_0} and I_{t_1} in a change detection perspective.

When considering the evolution of pdf issued from the joint SEM mixture estimation, only one map is to be considered and so an unique class ω'' for each pixel (i, j) . Then, the

TABLE I
MASS ASSIGNMENT FOR COMPARING I_{t_0} AND I_{t_1} .

Hypothesis	mass
\emptyset	0 (by definition)
θ_{ch}	$(1 - \rho(f^{t_0}(I_{t_0}(i, j) \omega), f^{t_1}(I_{t_1}(i, j) \omega')) \times \mathcal{D}(f^{t_0}(I_{t_0}(i, j) \omega), f^{t_1}(I_{t_1}(i, j) \omega'))$
$\theta_{\text{no ch}}$	$\rho(f^{t_0}(I_{t_0}(i, j) \omega), f^{t_1}(I_{t_1}(i, j) \omega')) \times (1 - \mathcal{D}(f^{t_0}(I_{t_0}(i, j) \omega), f^{t_1}(I_{t_1}(i, j) \omega'))$
$\theta_{\text{ch} \cap \text{no ch}}$	$\rho(f^{t_0}(I_{t_0}(i, j) \omega), f^{t_1}(I_{t_1}(i, j) \omega')) \times \mathcal{D}(f^{t_0}(I_{t_0}(i, j) \omega), f^{t_1}(I_{t_1}(i, j) \omega'))$
$\theta_{\text{ch} \cup \text{no ch}}$	$(1 - \rho(f^{t_0}(I_{t_0}(i, j) \omega), f^{t_1}(I_{t_1}(i, j) \omega')) \times (1 - \mathcal{D}(f^{t_0}(I_{t_0}(i, j) \omega), f^{t_1}(I_{t_1}(i, j) \omega'))$

TABLE II
MASS ASSIGNMENT FOR COMPARING I_{t_0} AND I_{t_1} INTO THE JOINT SEGMENTATION.

Hypothesis	mass
\emptyset	0 (by definition)
θ_{ch}	$\rho(f_{t_0}^{t_0, t_1}(I_{t_0}(i, j) \omega''), f_{t_1}^{t_0, t_1}(I_{t_1}(i, j) \omega'')) \times \mathcal{D}(f_{t_0}^{t_0, t_1}(I_{t_0}(i, j) \omega''), f_{t_1}^{t_0, t_1}(I_{t_1}(i, j) \omega'')) \times \mathcal{S}(f_{t_0}^{t_0, t_1}(I_{t_0}(i, j) \omega''), f_{t_1}^{t_0, t_1}(I_{t_1}(i, j) \omega''))$
$\theta_{\text{no ch}}$	$(1 - \rho(f_{t_0}^{t_0, t_1}(I_{t_0}(i, j) \omega''), f_{t_1}^{t_0, t_1}(I_{t_1}(i, j) \omega'')) \times (1 - \mathcal{D}(f_{t_0}^{t_0, t_1}(I_{t_0}(i, j) \omega''), f_{t_1}^{t_0, t_1}(I_{t_1}(i, j) \omega'')) \times (1 - \mathcal{S}(f_{t_0}^{t_0, t_1}(I_{t_0}(i, j) \omega''), f_{t_1}^{t_0, t_1}(I_{t_1}(i, j) \omega''))$
$\theta_{\text{ch} \cap \text{no ch}}$	$m(\theta_{\text{ch} \cap \text{no ch}})^*$
$\theta_{\text{ch} \cup \text{no ch}}$	$\rho(f_{t_0}^{t_0, t_1}(I_{t_0}(i, j) \omega''), f_{t_1}^{t_0, t_1}(I_{t_1}(i, j) \omega'')) \times (1 - \mathcal{D}(f_{t_0}^{t_0, t_1}(I_{t_0}(i, j) \omega''), f_{t_1}^{t_0, t_1}(I_{t_1}(i, j) \omega'')) \times \mathcal{S}(f_{t_0}^{t_0, t_1}(I_{t_0}(i, j) \omega''), f_{t_1}^{t_0, t_1}(I_{t_1}(i, j) \omega''))$

* $m(\theta_{\text{ch} \cap \text{no ch}})$ is adjusted in order to respect eq. (1).

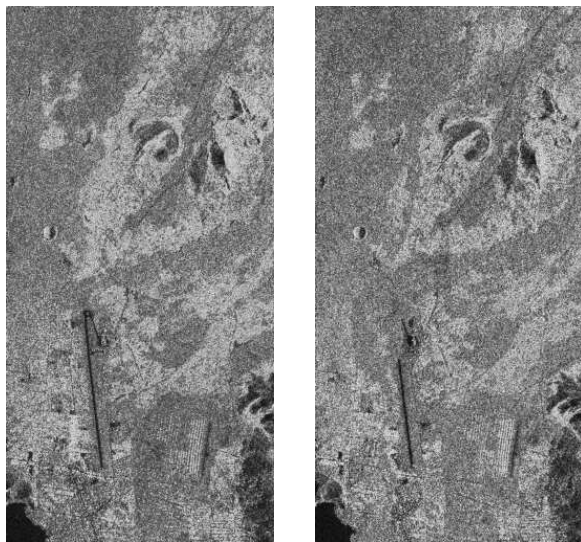
significance measurement of a pixel may be use to reduce ambiguity. The mass assignment is proposed in table II.

Finally, the decision is taken through the maximum of credibility, *i.e.* when $\text{Bel}(\theta_{\text{ch}}) > \text{Bel}(\theta_{\text{no ch}})$.

V. RESULTS

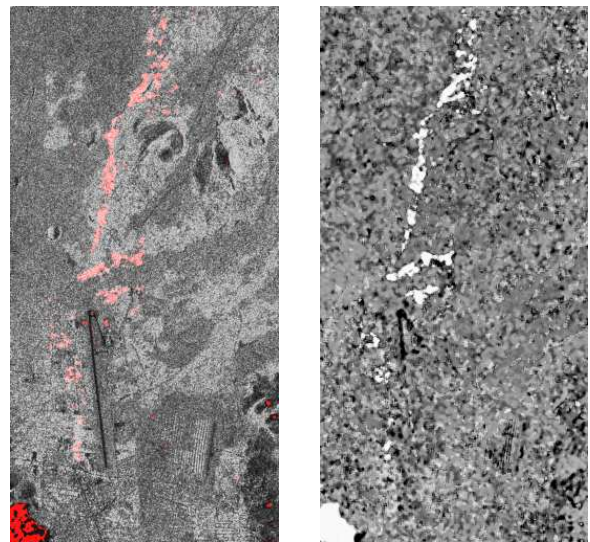
The technic is now illustrated with the couple of images in Fig. 1 which shows RADARSAT images acquired before and after an eruption of the Nyiragongo volcano (R.D. Congo) that occurred in January 2002. The (a) image comes from archive data (F5 mode) whereas the (b) image is a F2 beam.

Fig. 2 shows the results of decision making on the maximum of belief by using the two sources of evidences shown previously. It appears that even if changes were not fully detected, there are almost no false alarm. Even if this method takes a strong decision, it is possible to analyse the belief response or the interval [credibility, plausibility] to introduce a confident interval into the decision (as in most of DS applications). In the example shown, the top of the airport runway has been



(a) image I_{t_0} (b) image I_{t_1}

Fig. 1. Images to be used for change detection.



(a) Decision: $\text{Bel}(\theta_{\text{ch}}) > \text{Bel}(\theta_{\text{no ch}})$ (b) Belief on change: $\text{Bel}(\theta_{\text{ch}})$

Fig. 2. Change detection results (better seen in color).

covered by lava or mud but has not been affected to θ_{ch} . In fact, the analysis of the confident interval shows a high degree of uncertainty in the decision process. An additional source of evidence may then be used to help decision...

VI. CONCLUSION

Change detection in multitemporal SAR images is a challenging problem since thematic changes that have to be detected are hidden by several sensor-inherent and application-dependent factors such as ascending or descending orbit, several incidences, strong speckle noise... In this work, the joint characterization method do not consider pixel-based changes, but rather thematic changes as a modification of both spatial and temporal distributions of classes in the images. The proposed solution is based on the analysis of the evolution of the pdf yielded by the segmentation procedures to detect ground changes. The results we obtained are encouraging and the method should be further tested by using data sets with ground truth and associated to different sources of evidence.

It is important to note that this technique remains valid for multivariate (i.e. more than two dates) change detection problems, and can even help to automatically decide when the change occurs in a sequence of several 'before' and several 'after' images.

ACKNOWLEDGMENT

Authors would like to thank the French Space Agency (CNES) for the RADARSAT images, under contract CNES R&T (*Études de Détection de Changements entre images SAR*), 2003.

REFERENCES

[1] L. Boschetti, "A multitemporal algorithm for burned area detection in Mexican woodland and shrubland environment with SPOT-VEGETATION data," in *Proc. of the IEEE Geoscience and Remote Sensing Symp. (IGARSS 2003)*, Toulouse, France, July 2003.

[2] J.-F. Mas, "Monitoring land-cover changes: a comparison of change detection techniques," *Int. J. of Remote Sensing*, vol. 20, no. 1, pp. 139–152, 1999.

[3] A. A. Nielsen, K. Conradsen, and J. J. Simpson, "Multivariate alteration detection (MAD) and MAF processing in multispectral, bitemporal image data: new approaches to change detection studies," *Rem. Sens. Environ.*, vol. 64, no. 1, pp. 1–19, 1998.

[4] R. Wiemker, "An iterative spectral-spatial bayesian labeling approach for unsupervised robust change detection on remotely sensed multispectral imagery," in *Proc. of the 7th Int. Conf. on Computer Analysis of Images and Patterns (CAIP 1997)*, Kiel, Germany, Sept. 1997, pp. 263–270.

[5] P. R. Coppin, I. G. Jonckheere, and K. Nachaerts, "Digital change detection in ecosystem monitoring : a review," *Int. J. of Remote Sensing*, vol. 24, pp. 1–33, 2003.

[6] J. Inglada, "Change detection on SAR images by using a parametric estimation of the Kullback-Leibler divergence," in *Proc. of the IEEE Geoscience and Remote Sensing Symp. (IGARSS 2003)*, Toulouse, France, July 2003.

[7] L. Bruzzone and D. F. Prieto, "Automatic analysis of the difference image for unsupervised change detection," *IEEE Trans. Geosci. Remote Sensing*, vol. 38, no. 3, pp. 1171–1182, May 2000.

[8] F. T. Bujor, J.-M. Nicolas, E. Trouvé, and J.-P. Rudant, "Application of log-cumulants to change detection in multi-temporal SAR images," in *Proc. of the IEEE Geoscience and Remote Sensing Symp. (IGARSS 2003)*, vol. 2, Toulouse, France, July 2003, pp. 1386–1388.

[9] S. Derrode, G. Mercier, and W. Pieczynski, "Unsupervised change detection in SAR images using a multicomponent HMC model," in *Proc. of the 2nd Int. Workshop on the Analysis of Multitemporal Remote Sensing Images (Multi-Temp 2003)*, Ispra, Italy, July 2003.

[10] V. P. Onana, E. Trouvé, G. Mauris, J.-P. Rudant, and P.-L. Frison, "Change detection in urban context with multitemporal ERS-SAR images by using data fusion approach," in *Proc. of the IEEE Geoscience and Remote Sensing Symp. (IGARSS 2003)*, Toulouse, France, July 2003.

[11] J. Inglada, "Similarity measures for multisensor remote sensing images," in *Proc. of the IEEE Geoscience and Remote Sensing Symp. (IGARSS 2002)*, Toronto, Canada, June 2002.

[12] P. Deer, "Digital change detection in remotely sensed imagery using fuzzy set theory," PhD, Univ. of Adelaide, Australia, 1998.

[13] A. Singh, "Digital change detection techniques using remotely-sensed data," *Int. J. of Remote Sensing*, vol. 10, pp. 989–1003, 1989.

[14] F. Smarandache and J. Dezert, *Advances and Applications of DSMT for Information Fusion*. Rehoboth, USA: American Research Press, 2004, <http://www.gallup.unm.edu/~smarandache/DSMT-book1.pdf>.